Geophysical Research Letters

RESEARCH LETTER
10.1029/2023GL103524

Special Section:
Hydrogeodesy: Understanding changes in water resources using space geodetic observations

Key Points:
- High-resolution Sentinel-2 images and daily in situ water levels were used to estimate reservoir sedimentation rates and capacity losses
- Estimated reservoir sedimentation rates and storage capacity losses have a mean error of 0.05% yr^{-1} of full storage capacity
- Potential applications of this method to ungauged reservoirs are feasible with sub-monthly level data from recent satellite altimeters

Supporting Information:
Supporting Information may be found in the online version of this article.

Correspondence to:
F. Yao,
fangfang.yao@colorado.edu;
yaoff.luke@gmail.com

Citation:
Yao, F., Minear, J. T., Rajagopalan, B., Wang, C., Yang, K., & Livneh, B. (2023). Estimating reservoir sedimentation rates and storage capacity losses using high-resolution Sentinel-2 satellite and water level data. *Geophysical Research Letters*, *50*, e2023GL103524. https://doi.org/10.1029/2023GL103524

Received 6 MAR 2023
Accepted 27 JUL 2023

Author Contributions:
Conceptualization: Fangfang Yao
Formal analysis: Fangfang Yao
Funding acquisition: Fangfang Yao
Methodology: Fangfang Yao, J. Toby Minear, Balaji Rajagopalan, Chao Wang

Estimating Reservoir Sedimentation Rates and Storage Capacity Losses Using High-Resolution Sentinel-2 Satellite and Water Level Data

Fangfang Yao[1,2], J. Toby Minear[1], Balaji Rajagopalan[1,3], Chao Wang[4], Kehan Yang[5,6], and Ben Livneh[1,3]

[1]Cooperative Institute for Research in Environmental Sciences (CIRES), University of Colorado Boulder, Boulder, CO, USA, [2]Environmental Institute, University of Virginia, Charlottesville, VA, USA, [3]Department of Civil, Environmental and Architectural Engineering, University of Colorado Boulder, Boulder, CO, USA, [4]Department of Earth, Marine and Environmental Sciences, University of North Carolina at Chapel Hill, Chapel Hill, NC, USA, [5]Department of Civil & Environmental Engineering, University of Washington, Seattle, WA, USA, [6]eScience Institute, University of Washington, Seattle, WA, USA

Abstract In nearly all reservoirs, storage capacity is steadily lost due to trapping and accumulation of sediment. Despite critical importance to freshwater supplies, reservoir sedimentation rates are poorly understood due to sparse bathymetry survey data and challenges in modeling sedimentation sequestration. Here, we proposed a novel approach to estimate reservoir sedimentation rates and storage capacity losses using high-resolution Sentinel-2 satellites and daily in situ water levels. Validated on eight reservoirs across the central and western United States, the estimated reservoir bathymetry and sedimentation rates have a mean error of 4.08% and 0.05% yr^{-1}, respectively. Estimated storage capacity losses to sediment vary among reservoirs, which overall agrees with the pattern from survey data. We also demonstrated the potential applications of the proposed approach to ungauged reservoirs by combining Sentinel-2 with sub-monthly water levels from recent satellite altimeters.

Plain Language Summary Reservoir storage capacity is steadily lost due to sediment filling, which threatens freshwater supplies both now and in the future. Yet, lost reservoir storage capacities to sediment are largely unknown. Here, we develop a generic method to estimate capacity losses and reservoir sedimentation rates by leveraging remote sensing techniques. We tested on eight reservoirs across the central and western United States and found capacity losses and sedimentation rates vary across reservoirs. The proposed method offers a promising alternative to evaluate and predict capacity losses in reservoirs nationwide and globally, and thus supports effective water managements and planning for sustainable freshwater supplies in the future.

1. Introduction

For thousands of years humans have relied on reservoirs—regulated natural lakes and humanmade ones, for water supply, irrigation, and more recently hydropower generation (Lehner et al., 2011). The cumulative storage capacity of global reservoirs now reaches over 8,000 km^3, which is roughly twice as much as the global annual river runoff (Wang et al., 2022). By regulating river flow, these reservoirs make a notable contribution to global water, food, and energy security and to reducing flood risks. For example, reservoirs provide more than 40% of global irrigation water (Biemans et al., 2011).

Reservoir storage capacity is steadily being lost to the gradual accumulation of the incoming sediment load from rivers, which is due to the reducing velocity in the connection between rivers and the reservoir with limited force to move sediment particles (Asthana & Khare, 2022). Sediment-induced reservoir capacity losses accumulate over time and are particularly notable in aging reservoirs. For example, in the United States, a recent study used an upscaling method and estimated that reservoir storage per capita has declined by over one-third with a wide range of uncertainty during the past 50 years as a combined result of sedimentation and population growth (Randle et al., 2021). Additionally, sedimentation rates can vary substantially from one reservoir to another owing to a number of factors, such as soil, land cover, land disturbance (e.g., landslides and wildfires), contributing area, and hydroclimate (Obialor et al., 2019; Sankey et al., 2017). Accurate knowledge of reservoir sedimentation rates is critical for sustainable water resources management, both now and in the future.

Validation: Fangfang Yao, J. Toby Minear
Visualization: Fangfang Yao, Kehan Yang, Ben Livneh
Writing – original draft: Fangfang Yao
Writing – review & editing: Fangfang Yao, J. Toby Minear, Balaji Rajagopalan, Chao Wang, Kehan Yang, Ben Livneh

Sedimentation rates are poorly monitored due to observation and modeling challenges. The most direct measurement is through periodic lake bathymetry surveys. For example, surveys at two different times are often used to estimate the volume loss to sediment during the period. Owing to time-consuming and expensive, bathymetry survey data is spatially sparse and often not publicly available (Foteh et al., 2018). Sedimentation rates can also be estimated through process-based models (Doten et al., 2006; Minear & Kondolf, 2009). However, the lack of sedimentation and auxiliary data for model calibration and parameterization often lead to high uncertainties in modeled estimates (Trimble, 1999). Empirical methods, such as the Modified Universal Soil Loss Equation (Weifeng & Bingfang, 2008; J. R. Williams & Berndt, 1977) or the Monovariate Rating Curve (Glysson, 1987), are derived from observed data informed by sediment physics and are widely used due to their computational efficiency. However, they suffer from representing catchment systems homogeneously and estimating outputs based on a single event (Pechlivanidis et al., 2011). Recent advancements combine land surface models with these empirical models to model space-time variability of sedimentation (e.g., Stewart et al., 2017). Limited data, calibration, and parametrization inhibit them from widespread applications.

Due to data scarcity and modeling uncertainties, researchers have attempted to estimate reservoir sedimentation rates using satellite-derived sediment fluxes in rivers flowing to reservoirs or lake bathymetry. River sediment load retrieved from satellite-observed turbidity can be combined with trap efficiency models (Brune, 1953; Moragoda et al., 2023) to predict the volume of trapped sediment in reservoirs (Condé et al., 2019; Dethier et al., 2020; Pham et al., 2018). However, remotely sensed estimates on river sediment load have insufficient spatial or temporal resolutions to estimate the total amount of sediment trapped in a reservoir (Condé et al., 2019; Gardner et al., 2023). Alternatively, satellite observations of time-varying water area changes and water level data (e.g., from in-situ gauges) can be combined to construct recent lake bathymetry and estimate storage losses (Foteh et al., 2018; Jagannathan & Krishnaveni, 2021; Pandey et al., 2016; Tesfaye et al., 2023). Foteh et al. (2018) used the constructed bathymetry from 30-m Landsat images and in-situ levels to estimate actual reservoir storage in 2017 and then compared it with the designed storage in 1975 to deduce the volume of trapped sediment in Jayakwadi Reservoir in India over the past five decades. However, most of these satellite-based attempts focused on analyzing one single reservoir (Table S1 in Supporting Information S1), lacking an accurate assessment of their applicability to regional scales. This limitation is crucial as it hinders our understanding of the variations in sediment rates, as well as the underlying sediment processes and environmental factors (Atulley et al., 2022). This is particularly concerning for two main reasons. First, is the uncertainty in mapped water area changes due to the relatively coarse spatial resolution of Landsat satellites and challenges in mapping water area changes due to factors, such as the disturbance of clouds, shadows, and aquatic vegetation. Second is that the derived lake bathymetry often only covers a small fraction of the full bathymetry due to insufficient frequency of cloud-free observations of Landsat satellites (e.g., monthly to yearly) in a given period. As a result, reservoir sedimentation rates at regional to global scales remain largely unknown.

The European Space Agency's Sentinel-2 mission with two satellites launched in 2015 and 2017, respectively, observes Earth's surface at a 10-m resolution with a sub-weekly frequency. These satellites provide new opportunities for estimating lake bathymetry when combined with water levels. Compared to Landsat observations, Sentinel-2 enables mapping of water areas at higher spatial and temporal resolutions (Topaloğlu et al., 2016), which allows for more accurate estimates of water area changes at a wider range of water levels. In addition, recent advances in satellite altimeters bring new opportunities to track water levels from space. More advanced radar altimeters, such as Sentinel-3 altimetry (2016—the present) and Surface Water and Ocean Topography (SWOT, launched in 2022), can observe water levels in both large and small water bodies (<10 to >100,000 km^2) with up to 10-cm accuracy at a sub-monthly frequency owing to advanced Synthetic Aperture Radar mode or wide-swath technology (Biancamaria et al., 2016). While satellite altimeters have the potential to substitute daily in-situ levels, however, whether the revisit frequency of satellite altimetry is sufficient for monitoring reservoir sedimentation rates has never been tested.

Here, we develop and evaluate a novel approach for estimating reservoir sedimentation rates using 10-m Sentinel-2 satellites and daily in situ water levels. We validate estimated sedimentation rates against reference rates from sedimentation surveys over eight reservoirs, with various sizes and other characteristics, across the central and western US. We test the performance of the proposed approach not only on continuous daily water level data, but also on filtered water levels via the revisit frequency of the Sentinel-3 altimeter. This study provides the first large-scale evaluation of satellite-based estimates of reservoir sedimentation rates and offers insights into

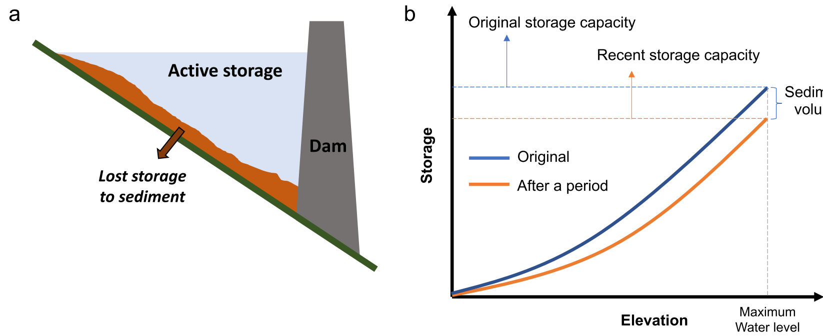

Figure 1. Illustration of reservoir sedimentation and storage capacity loss. (a) Reservoir profile with sedimentation highlighted. (b) Elevation-storage curve (i.e., stage-capacity curve) for original and recent periods. Differences in storage for the same elevation are the result of sediment-driven changes to reservoir bathymetry—described in Section 2.3.

the feasibility of combining Sentinel-2 images with satellite altimeters for reservoir sedimentation studies when in-situ water levels are not available.

2. Materials and Methods

We identified eight reservoirs with sedimentation survey data for testing the performance of our proposed methodology across the western and central US based on their sizes and geographic and climatic characteristics (Figure S1 in Supporting Information S1), as well as the availability of bathymetry survey data from the United States Bureau of Reclamation (USBR). For each reservoir, we first collected daily in situ water levels from gauging stations. Next, we mapped the initial water extents from Sentinel-2 images during the period 2015—2022. We ranked the initial water extents based on water level and refined water areas based on the topographic constraint of lake growth and shrinkage. The time-varying water areas and levels were combined to derive the lake bathymetry during 2015–2022, which was used to estimate the near-present storage capacity. Finally, we estimated the sediment volume and sedimentation rate based on the difference between the near-present storage capacity and the original maximum storage in design—shown in the schematic in Figure 1.

2.1. Obtaining Water Levels

Daily in situ water levels were obtained from federal agencies, including the United States Geological Survey (USGS), and the USBR (Table 1). As satellite-derived water level data are currently unavailable for studied reservoirs, we created another set of water levels through resampling the daily water levels at the temporal revisit frequency (27-day) of the Sentinel-3 altimeter. We selected Sentinel-3 because of its high resolution with a footprint size of 300 m, sub-monthly temporal frequency, and temporal record covering nearly entire Sentinel-2 era (2015—2022) (Taburet et al., 2020). Sentinel-3-derived lake levels have a reported error of 0.2 m (Gao et al., 2019). We simulated this source of error in the 27-day water levels, assuming a uniform error distribution.

2.2. Mapping Water Areas

We followed the methodology from Yao et al. (2019) to map and refine water areas from Sentinel-2 images. The detailed procedures are introduced in Supporting Information S1. In brief, an ensemble of sets of initial water

Table 1
A Summary of Data Sets Used in This Study

Data set	Spatial resolution	Temporal resolution	Temporal coverage	Source or reference
Sentinel-2 images	10-m	16-day	2015 to the present	Drusch et al. (2012)
In-situ water levels	N/A	Daily	Varies	USBR, USGS
Sentinel-3 altimetry	300-m	27-day	2016 to the present	Donlon et al. (2012)
In situ bathymetry survey	Sub-meter	Irregular interval, once per 26 years on average	Varies	USBR

extents was mapped from different water spectral indices, including the Normalized Difference Water Index (NDWI) (McFeeters, 1996), the Modified Normalized Difference Water Index (Xu, 2006), the High Resolution Water Index (Yao et al., 2015), the 2015 Water Index (WI2015) (Fisher et al., 2016), and two Automatic Water Extraction Indices (AWEInsh and AWEIsh) (Feyisa et al., 2014) (see Table S3 in Supporting Information S1 for their configurations). The best set of initial water extents was identified as the one which water areas achieve the strongest correlation with water levels. Mapping errors in the initial water extents were further reduced based on the topographic constraint. The initial water extents were ranked based on the level. We assumed that each water extent with a lower water surface elevation should be completely enclosed by a water extent with a higher elevation. For each water extent, two higher isobaths were used to remove commission errors that were identified as portions of "water" beyond both higher isobaths, while two lower isobaths were used to correct omission errors that were identified as "islands" being inundated in both lower isobaths (Yao et al., 2019). Our method cannot map water beneath the capony of trees. To evaluate this source of error, we calculated the tree cover in historical maximum inundation extent (1984—2021) (Pekel et al., 2016) of each studied lake using recent high-resolution Google Earth images.

2.3. Constructing Lake Bathymetry

The water areas and levels were paired by time, resulting in area-level duplets. Each level was paired with the water area on the same day when the continuous daily water level data was used. However, when using the simulated altimetry levels, we matched each level with the water area mapped at the closest date within a week to balance the tradeoff between differencing time and the number of area-level duplets. These area-level duplets were used to calibrate the hypsometric curve using a smoothing spline fit to preserve the observations as much as possible. However, if the used water level data did not capture the minimum and maximum levels associated with full storage capacity, the hypsometric curve needed to be extrapolated. As the smoothing spline fits have limited predictive skill beyond the range of observations (Hastie et al., 2009), we used different fitting methods for hypsometry extrapolation. To extrapolate toward the maximum level, we used a linear fit and the slope was calculated as the overall slope of area-level duplets within either the uppermost 10-ft section or the uppermost section over half of the extrapolated height, whichever is larger. Only area-level duplets in the upper proportion (above the 50th percentile in level) were used considering possible slope variability in the lower proportion. To extrapolate toward the minimum level, that is, elevation of the streambed at the dam axis with a negligible water area (assumed as zero), we followed existing studies (Crétaux et al., 2016; Wang et al., 2018) and used quadratic polynomial fitting to minimize overfitting due to limited data points. The hypsometry extrapolation may introduce additional uncertainty (Crétaux et al., 2016), which was assessed during the validation.

2.4. Estimating Reservoir Sedimentation Rates and Validation

We calculated the near-present storage capacity via the integral of the area-level curve $h(A, L)$ from the minimum water level (L_0) to the maximum level ($L_{\max}$) using Equation 1. The original storage capacity in design was obtained from the USBR reservoir reports, which was calculated based on a bathymetry survey near the dam completion year. The sediment-induced reservoir storage capacity loss was calculated as the residual between the original storage capacity in design and the near-present storage capacity (Figure 1b). The overall sedimentation rate was calculated as the amount of sediment volume per year relative to the original storage capacity. To validate the estimated sedimentation rates, we generated reference sedimentation rates using the latest sedimentation survey for each reservoir. All studied reservoirs have at least one survey since 2005. The sedimentation survey data were collected from the USBR. Errors in sedimentation rates are assessed using absolute errors (AE) and normalized errors (NE) calculated as the ratio of the AE and full storage capacity.

$$\text{Stoarage capacity} = \int_{L_0}^{L_{\max}} h(A, L)\,dL \tag{1}$$

3. Results

3.1. Evaluation of Satellite-Derived Bathymetry and Sediment Estimates

Satellite-estimated reservoir sedimentation rates show a mean bias of 0.05% yr^{-1} (Figure 2), which is much smaller than the mean sedimentation rate (0.18% yr^{-1}) from survey data. However, the errors of estimated

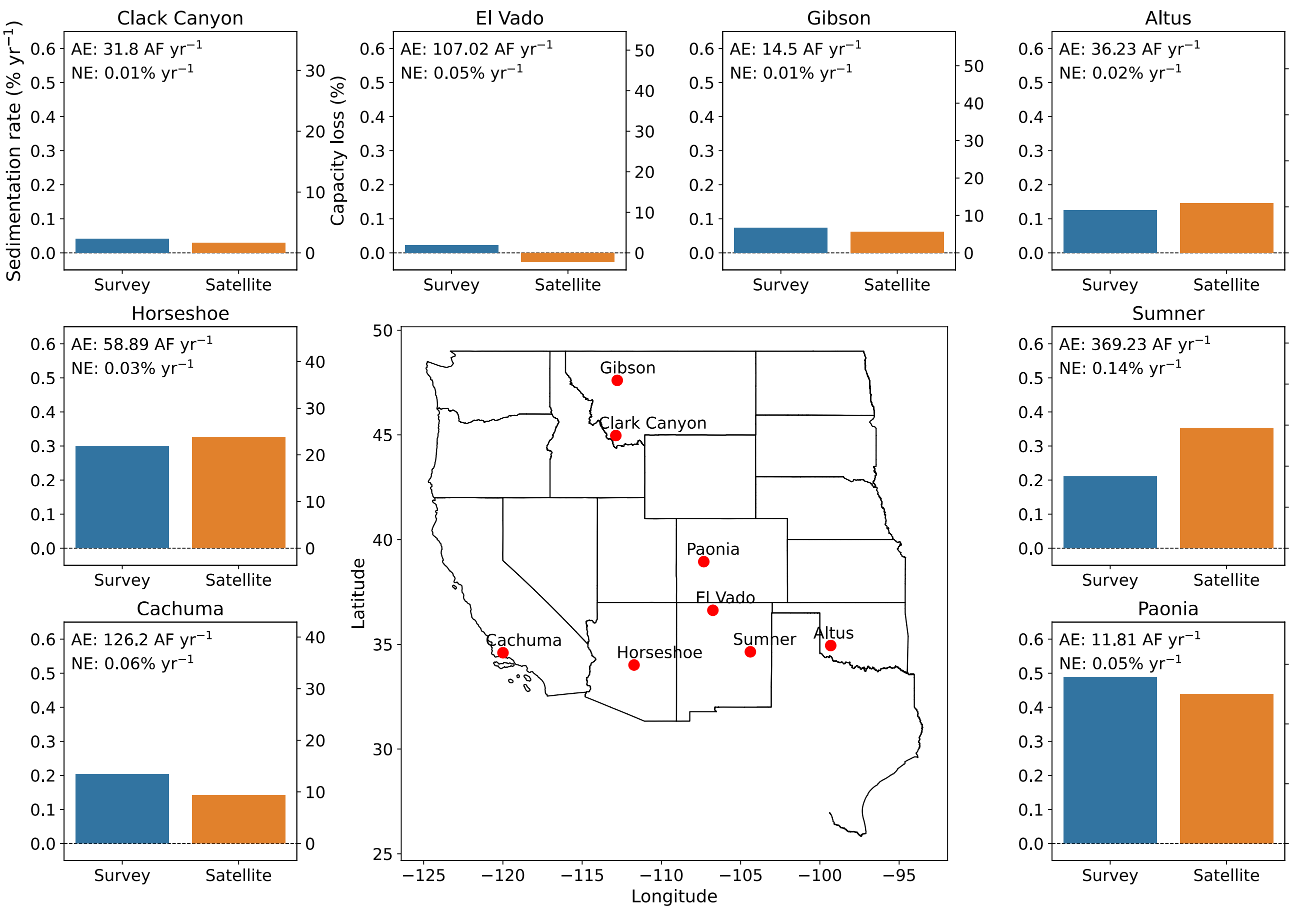

Figure 2. Comparison of estimated sedimentation rates and storage capacity losses against reference data from surveys on eight reservoirs across the central and western US. Actual Error (AE) and Normalized Error (NE) are shown in each bar plot. NE was calculated as the ratio of AE and full storage capacity. AF is acer-ft and 1 AF is equivalent to 1,233.48 m^3.

sedimentation rate vary among reservoirs due to different accuracy of satellite-derived bathymetry. The derived bathymetry has a mean percent bias of 4.08%, with lowest in Lake Gibson (0.31%) and highest in Lake Sumner (15.66%) (Figure 3). Sedimentation errors are relatively large in Summer (0.14%), Cachuma (0.06%), Paonia (0.05%), El Vado (0.05%), and Horseshoe (0.03% yr^{-1}) Lakes. For most (80%) of these reservoirs, the derived bathymetry has a percent bias larger than 3% (Table S2 in Supporting Information S1). There are a few factors contributing to the biases in bathymetry. First is the low exposure level of the bathymetry observed by satellites, particularly in high water levels. For example, the extrapolated fractions in the upper bathymetry are high in Lake Horseshoe (33%) and Lake Sumner (45%) (Table S2 in Supporting Information S1) and introduce large uncertainties (Figures 3e and 3f) (Crétaux et al., 2016). Second, there are trees in the riparian zone that are occasionally submerged (Figure S2 in Supporting Information S1). The tree covers in the historical inundation area are the highest in Lake Horseshoe (3.1%) and Lake Sumner (2.7%) (Table S2 in Supporting Information S1). The mapping error due to tree disturbance is amplified when extrapolating a significant fraction toward the maximum reservoir level (Figures 3e and 3f). Third is the shifted lowest elevation (i.e., minimum level with a non-zero area) due to complete filling by sediment. The lowest elevations were shifted significantly in Paonia (76), Horseshoe (62), Sumner (48), and Cachuma (43 ft) Lakes. Lake Horseshoe is less impacted by this source of uncertainty because its new lowest elevation was observed by satellites (Figure 3e). The mean absolute error of sedimentation rates is 94.46 acer-ft yr^{-1} or 116,514.52 m^3 yr^{-1}. Lake Sumner also has the largest absolute error (369.23 acer-ft yr^{-1}), followed by Lake Cachuma (126.20), El Vado (107.02), and Horseshoe (58.89 acer-ft yr^{-1}).

Despite the uncertainty, the patterns of estimated sedimentation rates and storage capacity losses are overall consistent with that of reference rates from surveys (Figure 2), suggesting the applicability of the proposed approach for estimating regional variability in sedimentation rates. For example, both satellite and survey

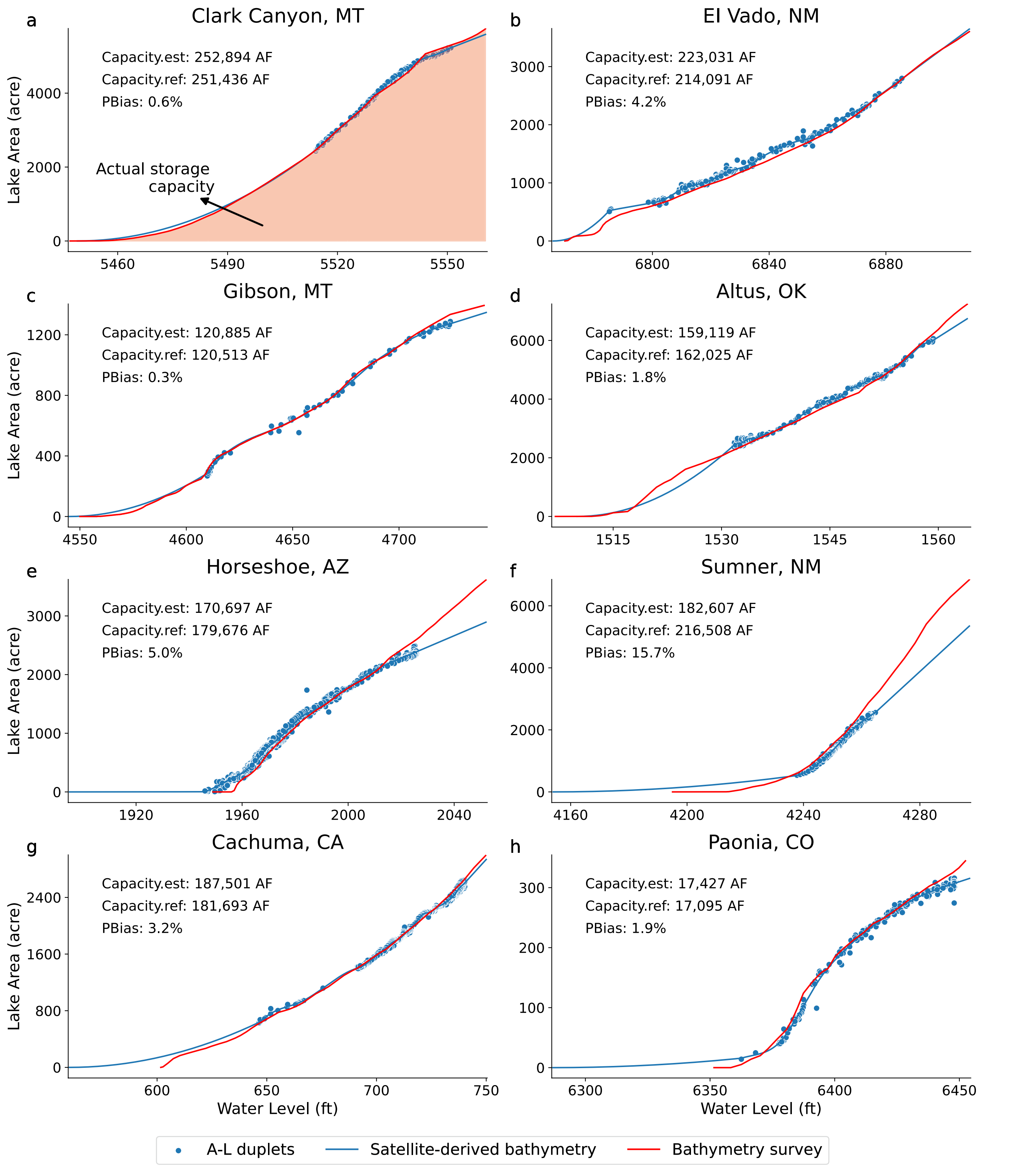

Figure 3. Validation of satellite-derived bathymetric curve and storage capacity against bathymetry survey for eight US reservoirs. (a) Lake Clark Canyon, Montana, MT, (b) Lake El Vado, New Mexico, NM, (c) Lake Gibson, MT, (d) Lake Altus, Oklahoma, OK. (e) Lake Horseshoe, Arizona, AZ, (f) Lake Sumner, NM, (g) Lake Cachuma, California, CA, and (h) Lake Paonia, Colorado, CO. Shading in panel (a) represents the actual storage capacity based on the latest survey.

estimates indicate high sedimentation rates in Lake Paonia and Lake Horseshoe and lower sedimentation rates in Lake Clark Canyon and Lake El Vado. Lake Paonia lost 27% of its full storage capacity to sediment since filling, which is the highest among these reservoirs. In contrast, sediment-induced storage losses in Clark Canyon and El Vado are less than 5%. These estimates provide useful information of sedimentation rates and storage capacity losses for reservoir management and predicting future freshwater storage capacity.

3.2. Potential for Estimating Reservoir Sedimentation Using Satellite Imagery and Altimeters

Satellite altimetry provides an alternative to monitor inland water levels when in-situ measurements are unavailable. Here, we examine whether the 27-day observation frequency of Sentinel-3 altimeter is sufficient for estimating reservoir sedimentation. By testing on the simulated Sentinel-3 water levels, we found that estimated reservoir sedimentation rates from satellite data alone have a mean error of 0.05% yr^{-1} or 101.21 acer-ft yr^{-1}, which is close to reported errors (0.05% yr^{-1} and 94.46 acer-ft yr^{-1}) using daily level data. Estimated reservoir sedimentation rates from the 27-day levels are quite comparable to those estimated from daily in-situ levels with an R^2 value of 0.995 and an RMSE of 0.01% yr^{-1} (Figure S3 in Supporting Information S1).

4. Discussion

Despite the significant issue of sedimentation, in-situ survey data is spatially sparse, inconsistent in time, and often is not publicly available nor up to date. The proposed method leverages high spatiotemporal Sentinel-2 satellites (10-m, sub-weekly), recent advances in water area mapping (Yao et al., 2019), and daily in situ levels to estimate near-present reservoir storage capacity and lost storage to sediment thus far. Validated on eight US reservoirs, our method achieves a mean error of 4.08% in estimating the near-present storage capacity and a mean error of 0.05% yr^{-1} for sedimentation rates. Different from most existing satellite-based approaches focusing on analyzing a single reservoir (e.g., Foteh et al., 2018; Jagannathan & Krishnaveni, 2021; Pandey et al., 2016) (Table S1 in Supporting Information S1), our method reveals that sedimentation rates vary among reservoirs, which overall agrees with the pattern from survey data. Thus, the proposed method offers new insights into the regional variations in sedimentation rates under different environmental settings and sediment processes (Atulley et al., 2022).

A prerequisite for the approach presented here is a wide range of reservoir levels during the Sentinel-2 era in order to alleviate the uncertainty of hypsometry extrapolation, although Bayesian regression approaches (e.g., Ossandón et al., 2021) may be employed to capture the uncertainty robustly. Extensive extrapolation in high water levels needs to be interpreted with care, particularly when compounded with additional disturbance of tree cover (Figure S2 in Supporting Information S1). Water levels in some reservoirs, for example, Lake Mead, on the Colorado River, were consistently low during recent years due to megadroughts (A. P. Williams et al., 2020; Xiao et al., 2018). Observations from Sentinel-2 are only able to capture water area changes in the lower storage proportion, which accounts for a small fraction of the full reservoir storage. We surmise that these reservoirs can only be estimated accurately once the drought conditions have eased and water levels are back to normal.

While this study primarily focuses on the total storage loss to sediment in reservoirs since their filling, the proposed approach may be applicable for estimating decadal variability in sedimentation rates when combined with longer-term Landsat missions. Visual examination of the results for Lake Horseshoe reveals new details on sedimentation over the past four decades (1983–2022) (Figure 4). For example, the lowest elevation has been elevated due to complete filling by sediment in near-bottom storage. The bathymetric curve shows a consistently downward shift over time. The sedimentation rate decreased over the period 1983–2022, which is possibly linked to the declines in total precipitation and extreme precipitation (Figure S4 in Supporting Information S1). This suggests that the estimated time-varying sediment rates and trends can be used to understand and predict freshwater storage capacity losses under ongoing climate change and other land disturbances such as landslides (Qiankun et al., 2022; Tsai et al., 2012).

This study also shows the possibility of estimating sedimentation rates in ungauged reservoirs by incorporating sub-monthly level measurements from recent satellite altimeters, such as Sentinel-3 and SWOT. Estimated reservoir sedimentation rates from simulated levels at the temporal frequency of Sentinel-3 are overall comparable to those estimated from daily in situ levels (Figure S3 in Supporting Information S1), indicating the potential of estimating reservoir sedimentation rates using satellite data alone. In particular, SWOT satellite can provide

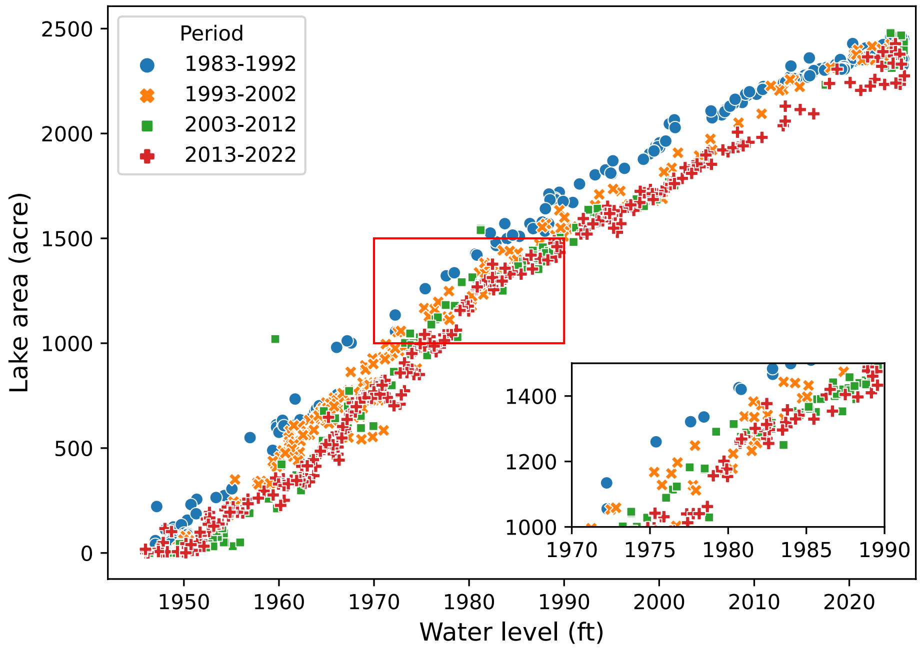

Figure 4. Estimated lake bathymetry over time (1982–2022) for Lake Horseshoe, AZ using Landsat images and daily in situ levels. The inset shows an enlarged view of the area-level duplets in the red box.

sub-monthly water levels with 10-cm (1σ) accuracy for water bodies larger than 1 ha (Biancamaria et al., 2016). Therefore, the proposed framework for estimating sediment sequestration in reservoirs will become more valuable when more high-quality water level products from satellites become available at regional to global scales. By estimating sedimentation rates in reservoirs nationwide and globally, the proposed novel method and potential extensions offer a powerful tool to inform water managers and policymakers on sustainable future freshwater supplies.

Data Availability Statement

The Sentinel-2 images were accessed from the Google Earth Engine platform at https://earthengine.google.com. In situ water level data were obtained from the USGS at https://waterdata.usgs.gov/nwis and the USBR at https://data.usbr.gov/time-series/search. Sedimentation survey data were provided by the USBR. The produced reservoir bathymetry and sedimentation data, and validation results are available at https://doi.org/10.5281/zenodo.8071451.

Acknowledgments

This research was supported by NOAA Cooperative Agreement with CIRES (NA17OAR4320101) and CIRES Innovative Research Program to F. Yao. Publication of this article was primarily funded by the University of Colorado Boulder Libraries Open Access Fund. We thank Tim Smith and Michael Diamond for proofreading this manuscript.

References

Asthana, B. N., & Khare, D. (2022). Reservoir sedimentation. In *Recent advances in dam engineering* (pp. 265–288). Springer. https://doi.org/10.1007/978-3-030-32278-6_12

Atulley, J. A., Kwaku, A. A., Gyamfi, C., Owusu-Ansah, E. D. J., Adonadaga, M. A., & Nii, O. S. (2022). Reservoir sedimentation and spatiotemporal land use changes in their watersheds: The case of two sub-catchments of the White Volta Basin. *Environmental Monitoring and Assessment*, *194*(11), 809. https://doi.org/10.1007/s10661-022-10431-y

Biancamaria, S., Lettenmaier, D. P., & Pavelsky, T. M. (2016). The SWOT mission and its capabilities for land hydrology. *Surveys in Geophysics*, *37*(2), 307–337. https://doi.org/10.1007/s10712-015-9346-y

Biemans, H., Haddeland, I., Kabat, P., Ludwig, F., Hutjes, R. W. A., Heinke, J., et al. (2011). Impact of reservoirs on river discharge and irrigation water supply during the 20th century. *Water Resources Research*, *47*(3), W03509. https://doi.org/10.1029/2009WR008929

Brune, G. M. (1953). Trap efficiency of reservoirs. *Eos, Transactions American Geophysical Union*, *34*(3), 407–418. https://doi.org/10.1029/TR034i003p00407

Condé, R. D. C., Martinez, J. M., Pessotto, M. A., Villar, R., Cochonneau, G., Henry, R., et al. (2019). Indirect assessment of sedimentation in hydropower dams using MODIS remote sensing images. *Remote Sensing*, *11*(3), 314. https://doi.org/10.3390/rs11030314

Crétaux, J.-F., Abarca-del-Río, R., Bergé-Nguyen, M., Arsen, A., Drolon, V., Clos, G., & Maisongrande, P. (2016). Lake volume monitoring from space. *Surveys in Geophysics*, *37*(2), 269–305. https://doi.org/10.1007/s10712-016-9362-6

Dethier, E. N., Renshaw, C. E., & Magilligan, F. J. (2020). Toward improved accuracy of remote sensing approaches for quantifying suspended sediment: Implications for suspended-sediment monitoring. *Journal of Geophysical Research: Earth Surface*, *125*(7), e2019JF005033. https://doi.org/10.1029/2019JF005033

Donlon, C., Berruti, B., Buongiorno, A., Ferreira, M.-H., Féménias, P., Frerick, J., et al. (2012). The global monitoring for environment and security (GMES) Sentinel-3 mission. *Remote Sensing of Environment*, *120*, 37–57. https://doi.org/10.1016/j.rse.2011.07.024

Doten, C. O., Bowling, L. C., Lanini, J. S., Maurer, E. P., & Lettenmaier, D. P. (2006). A spatially distributed model for the dynamic prediction of sediment erosion and transport in mountainous forested watersheds. *Water Resources Research*, *42*(4), W04417. https://doi.org/10.1029/2004WR003829

Drusch, M., Del Bello, U., Carlier, S., Colin, O., Fernandez, V., Gascon, F., et al. (2012). Sentinel-2: ESA's optical high-resolution mission for GMES operational services. *Remote Sensing of Environment*, *120*, 25–36. https://doi.org/10.1016/j.rse.2011.11.026

Feyisa, G. L., Meilby, H., Fensholt, R., & Proud, S. R. (2014). Automated water extraction index: A new technique for surface water mapping using landsat imagery. *Remote Sensing of Environment*, *140*, 23–35. https://doi.org/10.1016/j.rse.2013.08.029

Fisher, A., Flood, N., & Danaher, T. (2016). Comparing Landsat water index methods for automated water classification in eastern Australia. *Remote Sensing of Environment*, *175*, 167–182. https://doi.org/10.1016/j.rse.2015.12.055

Foteh, R., Garg, V., Nikam, B. R., Khadatare, M. Y., Aggarwal, S. P., & Kumar, A. S. (2018). Reservoir sedimentation assessment through remote sensing and hydrological modelling. *Journal of the Indian Society of Remote Sensing*, *46*(11), 1893–1905. https://doi.org/10.1007/s12524-018-0843-6

Gao, Q., Makhoul, E., Escorihuela, M. J., Zribi, M., Seguí, P. Q., García, P., & Roca, M. (2019). Analysis of retrackers' performances and water level retrieval over the Ebro River Basin using Sentinel-3. *Remote Sensing*, *11*(6), 718. https://doi.org/10.3390/RS11060718

Gardner, J., Pavelsky, T. M., Topp, S., Yang, X., Ross, M. R. V., & Cohen, S. (2023). Human activities change suspended sediment concentration along rivers. *Environmental Research Letters*, *18*(6), 064032. https://doi.org/10.1088/1748-9326/acd8d8

Glysson, G. D. (1987). Sediment-transport curves. https://doi.org/10.3133/ofr87218

Hastie, T., Tibshirani, R., Friedman, J. H., & Friedman, J. H. (2009). *The elements of statistical learning: Data mining, inference, and prediction* (Vol. 2, pp. 1–758). Springer. https://doi.org/10.1007/978-0-387-84858-7

Jagannathan, S., & Krishnaveni, M. (2021). Longitudinal sediment profiling and capacity lost in reservoir using multidate Sentinel-2 images. *Journal of the Indian Society of Remote Sensing*, *49*(2), 317–323. https://doi.org/10.1007/s12524-020-01179-4

Lehner, B., Liermann, C. R., Revenga, C., Vörösmarty, C., Fekete, B., Crouzet, P., et al. (2011). High-resolution mapping of the world's reservoirs and dams for sustainable river-flow management. *Frontiers in Ecology and the Environment*, *9*(9), 494–502. https://doi.org/10.1890/100125

McFeeters, S. K. (1996). The use of the Normalized Difference Water Index (NDWI) in the delineation of open water features. *International Journal of Remote Sensing*, *17*(7), 1425–1432. https://doi.org/10.1080/01431169608948714

Minear, J. T., & Kondolf, G. M. (2009). Estimating reservoir sedimentation rates at large spatial and temporal scales: A case study of California. *Water Resources Research*, *45*(12), W12502. https://doi.org/10.1029/2007WR006703

Moragoda, N., Cohen, S., Gardner, J., Muñoz, D., Narayanan, A., Moftakhari, H., & Pavelsky, T. M. (2023). Modeling and analysis of sediment trapping efficiency of large dams using remote sensing. *Water Resources Research*, *59*(6), e2022WR033296. https://doi.org/10.1029/2022WR033296

Obialor, C. A., Okeke, O. C., Onunkwo, A. A., Fagorite, V. I., & Ehujuo, N. N. (2019). *Reservoir sedimentation: Causes, effects and mitigation*. International Journal of Advanced Academic Research, Sciences, Technology and Engineering.

Ossandón, Á., Rajagopalan, B., Lall, U., Nanditha, J. S., & Mishra, V. (2021). A Bayesian hierarchical network model for daily streamflow ensemble forecasting. *Water Resources Research*, *57*(9), e2021WR029920. https://doi.org/10.1029/2021WR029920

Pandey, A., Chaube, U. C., Mishra, S. K., & Kumar, D. (2016). Assessment of reservoir sedimentation using remote sensing and recommendations for desilting Patratu Reservoir, India. *Hydrological Sciences Journal*, *61*(4), 711–718. https://doi.org/10.1080/02626667.2014.993988

Pechlivanidis, I. G., Jackson, B. M., Mcintyre, N. R., & Wheater, H. S. (2011). Catchment scale hydrological modelling: A review of model types, calibration approaches and uncertainty analysis methods in the context of recent developments in technology and applications. *Global NEST Journal*, *13*(3), 193–214. https://doi.org/10.30955/gnj.000778

Pekel, J.-F., Cottam, A., Gorelick, N., & Belward, A. S. (2016). High-resolution mapping of global surface water and its long-term changes. *Nature*, *540*(7633), 418–422. https://doi.org/10.1038/nature20584

Pham, Q. V., Ha, N. T. T., Pahlevan, N., Oanh, L. T., Nguyen, T. B., & Nguyen, N. T. (2018). Using Landsat-8 images for quantifying suspended sediment concentration in Red River (Northern Vietnam). *Remote Sensing*, *10*(11), 1841. https://doi.org/10.3390/rs10111841

Qiankun, G., Aijuan, W., Wei, Q., Zhijie, S., Jiaguo, G., Dandan, W., & Lin, D. (2022). Changes in the characteristics of flood discharge and sediment yield in a typical watershed in the Hengduan Mountain Region, Southwest China, under extreme precipitation events. *Ecological Indicators*, *145*, 109600. https://doi.org/10.1016/j.ecolind.2022.109600

Randle, T. J., Morris, G. L., Tullos, D. D., Weirich, F. H., Kondolf, G. M., Moriasi, D. N., et al. (2021). Sustaining United States reservoir storage capacity: Need for a new paradigm. *Journal of Hydrology*, *602*, 126686. https://doi.org/10.1016/j.jhydrol.2021.126686

Sankey, J. B., Kreitler, J., Hawbaker, T. J., McVay, J. L., Miller, M. E., Mueller, E. R., et al. (2017). Climate, wildfire, and erosion ensemble foretells more sediment in western USA watersheds. *Geophysical Research Letters*, *44*(17), 8884–8892. https://doi.org/10.1002/2017GL073979

Stewart, J. R., Livneh, B., Kasprzyk, J. R., Rajagopalan, B., Minear, J. T., & Raseman, W. J. (2017). A multialgorithm approach to land surface modeling of suspended sediment in the Colorado Front Range. *Journal of Advances in Modeling Earth Systems*, *9*(7), 2526–2544. https://doi.org/10.1002/2017MS001120

Taburet, N., Zawadzki, L., Vayre, M., Blumstein, D., Le Gac, S., Boy, F., et al. (2020). S3MPC: Improvement on inland water tracking and water level monitoring from the OLTC onboard Sentinel-3 altimeters. *Remote Sensing*, *12*(18), 3055. https://doi.org/10.3390/rs12183055

Tesfaye, A. T., Moges, M. A., Moges, M. M., Worqlul, A. W., Defersha, D. T., & Wassie, A. B. (2023). Reservoir sedimentation evaluation using remote sensing and GIS approaches for the reservoirs in the upper Blue Nile Basin. *Sustainable Water Resources Management*, *9*(1), 23. https://doi.org/10.1007/s40899-022-00792-0

Topaloğlu, R. H., Sertel, E., & Musaoğlu, N. (2016). Assessment of classification accuracies of SENTINEL-2 and LANDSAT-8 data for land cover/use mapping. *The International Archives of the Photogrammetry, Remote Sensing and Spatial Information Sciences*, *41*, 1055–1059. https://doi.org/10.5194/isprs-archives-XLI-B8-1055-2016

Trimble, S. W. (1999). Decreased rates of alluvial sediment storage in the Coon Creek Basin, Wisconsin, 1975-93. *Science*, *285*(5431), 1244–1246. https://doi.org/10.1126/science.285.5431.1244

Tsai, Z.-X., You, G. J.-Y., Lee, H.-Y., & Chiu, Y.-J. (2012). Use of a total station to monitor post-failure sediment yields in landslide sites of the Shihmen reservoir watershed, Taiwan. *Geomorphology*, *139*, 438–451. https://doi.org/10.1016/j.geomorph.2011.11.008

Wang, J., Song, C., Reager, J. T., Yao, F., Famiglietti, J. S., Sheng, Y., et al. (2018). Recent global decline in endorheic basin water storages. *Nature Geoscience*, *11*(12), 926–932. https://doi.org/10.1038/s41561-018-0265-7

Wang, J., Walter, B. A., Yao, F., Song, C., Ding, M., Maroof, A. S., et al. (2022). GeoDAR: Georeferenced global dams and reservoirs dataset for bridging attributes and geolocations. *Earth System Science Data*, *14*(4), 1869–1899. https://doi.org/10.5194/essd-14-1869-2022

Weifeng, Z., & Bingfang, W. U. (2008). Assessment of soil erosion and sediment delivery ratio using remote sensing and GIS: A case study of upstream Chaobaihe River catchment, north China. *International Journal of Sediment Research*, *23*(2), 167–173. https://doi.org/10.1016/S1001-6279(08)60016-5

Williams, A. P., Cook, E. R., Smerdon, J. E., Cook, B. I., Abatzoglou, J. T., Bolles, K., et al. (2020). Large contribution from anthropogenic warming to an emerging North American megadrought. *Science*, *368*(6488), 314–318. https://doi.org/10.1126/science.aaz9600

Williams, J. R., & Berndt, H. D. (1977). Sediment yield prediction based on watershed hydrology. *Transactions of the ASAE*, *20*(6), 1100–1104. https://doi.org/10.13031/2013.35710

Xiao, M., Udall, B., & Lettenmaier, D. P. (2018). On the causes of declining Colorado river streamflows. *Water Resources Research*, *54*(9), 6739–6756. https://doi.org/10.1029/2018WR023153

Xu, H. (2006). Modification of normalised difference water index (NDWI) to enhance open water features in remotely sensed imagery. *International Journal of Remote Sensing*, *27*(14), 3025–3033. https://doi.org/10.1080/01431160600589179

Yao, F., Wang, C., Dong, D., Luo, J., Shen, Z., & Yang, K. (2015). High-resolution mapping of urban surface water using ZY-3 multi-spectral imagery. *Remote Sensing*, *7*(9), 12336–12355. https://doi.org/10.3390/rs70912336

Yao, F., Wang, J., Wang, C., & Crétaux, J.-F. (2019). Constructing long-term high-frequency time series of global lake and reservoir areas using Landsat imagery. *Remote Sensing of Environment*, *232*, 111210. https://doi.org/10.1016/j.rse.2019.111210

References From the Supporting Information

Allen, G. H., & Pavelsky, T. M. (2018). Global extent of rivers and streams. *Science*, *361*(6402), 585–588. https://doi.org/10.1126/science.aat0636

Avinash, G., & Chandramouli, P. N. (2018). Assessment of reservoir sedimentation using RS and GIS techniques-A case study of Kabini Reservoir, Karnataka, India. *International Research Journal of Engineering and Technology*, *5*(8), 630–635.

Dadoria, D., Tiwari, H. L., & Jaiswal, R. K. (2017). Assessment of reservoir sedimentation in Chhattisgarh state using remote sensing and GIS. *International Journal of Civil Engineering & Technology*, *8*(4), 8–12. Retrieved from http://www.iaeme.com/IJCIET/issues.asp?JType=IJCIET&VType=8&IType=4%20

Darama, Y., Selek, Z., Selek, B., Akgul, M. A., & Dagdeviren, M. (2019). Determination of sediment deposition of Hasanlar Dam using bathymetric and remote sensing studies. *Natural Hazards*, *97*(1), 211–227. https://doi.org/10.1007/s11069-019-03635-y

Daudt, R. C., Wulf, H., Hafner, E. D., Bühler, Y., Schindler, K., & Wegner, J. D. (2023). Snow depth estimation at country-scale with high spatial and temporal resolution. *ISPRS Journal of Photogrammetry and Remote Sensing*, *197*, 105–121. https://doi.org/10.1016/j.isprsjprs.2023.01.017

Garg, A. A., Shawul, A. A., & Chakma, S. (2020). Assessment of sedimentation and useful life of Tehri reservoir using integrated approaches of hydrodynamic modelling, satellite remote sensing and empirical curves. *Current Science*, *118*(3), 411. https://doi.org/10.18520/cs/v118/i3/411-420

Jain, S. K., Singh, P., & Seth, S. M. (2002). Assessment of sedimentation in Bhakra Reservoir in the western Himalayan region using remotely sensed data. *Hydrological Sciences Journal*, *47*(2), 203–212. https://doi.org/10.1080/02626660209492924

Katiyar, R., Garg, P. K., & Jain, S. K. (2006). Watershed prioritization and reservoir sedimentation using remote sensing data. *Geocarto International*, *21*(3), 55–60. https://doi.org/10.1080/10106040608542393

Li, J., & Sheng, Y. (2012). An automated scheme for glacial lake dynamics mapping using Landsat imagery and digital elevation models: A case study in the Himalayas. *International Journal of Remote Sensing*, *33*(16), 5194–5213. https://doi.org/10.1080/01431161.2012.657370

Mukherjee, S., Veer, V., Tyagi, S. K., & Sharma, V. (2007). Sedimentation study of Hirakud reservoir through remote sensing techniques. *Journal of Spatial Hydrology*, *7*(1), 122–130.

Narasayya, K., Roman, U. C., Sreekanth, S., & Jatwa, S. (2012). Assessment of reservoir sedimentation using remote sensing satellite imageries. *Asian Journal of Geoinformatics*, *12*(4), 711–718.

Ninija Merina, R., Sashikkumar, M. C., Rizvana, N., & Adlin, R. (2016). Sedimentation study in a reservoir using remote sensing technique. *Applied Ecology and Environmental Research*, *14*(4), 296–304. https://doi.org/10.15666/aeer/1404_296304

Otsu, N. (1979). A threshold selection method from gray-level histograms. *IEEE Transactions on Systems, Man, and Cybernetics*, *9*(1), 62–66. https://doi.org/10.1109/TSMC.1979.4310076

Prasad, N. R., Garg, V., & Thakur, P. K. (2018). Role of SAR data in water body mapping and reservoir sedimentation assessment. In *ISPRS annals of the photogrammetry, remote sensing and spatial information sciences* (Vol. 4, pp. 151–158). https://doi.org/10.5194/isprs-annals-IV-5-151-2018

Sheng, Y., Song, C., Wang, J., Lyons, E. A., Knox, B. R., Cox, J. S., & Gao, F. (2016). Representative lake water extent mapping at continental scales using multi-temporal Landsat-8 imagery. *Remote Sensing of Environment*, *185*, 129–141. https://doi.org/10.1016/j.rse.2015.12.041

Skakun, S., Wevers, J., Brockmann, C., Doxani, G., Aleksandrov, M., Batič, M., et al. (2022). Cloud Mask Intercomparison eXercise (CMIX): An evaluation of cloud masking algorithms for Landsat 8 and Sentinel-2. *Remote Sensing of Environment*, *274*, 112990. https://doi.org/10.1016/j.rse.2022.112990

Skariah, M., & Suriyakala, C. D. (2021). Gauging of sedimentation in Idukki reservoir, Kerala (1974–2019), and the impact of 2018 Kerala floods on the reservoir. *Journal of the Indian Society of Remote Sensing*, *49*(9), 2103–2112. https://doi.org/10.1007/s12524-021-01375-w

Tiwari, S., Verma, S., & Ghosh, S. (2016). Estimation of sedimentation rate of a reservoir using remote sensing data: A case study of tehri reservoir. *International Journal of Latest Trends in Engineering and Technology*, *7*(3), 245–253. https://doi.org/10.21172/1.73.534

Wagh, S., & Manekar, V. (2021). Assessment of reservoir sedimentation using satellite remote sensing technique (SRS). *Journal of The Institution of Engineers (India): Series A*, *102*(3), 851–860. https://doi.org/10.1007/s40030-021-00539-8

Wang, J., Sheng, Y., & Tong, T. S. D. (2014). Monitoring decadal lake dynamics across the Yangtze Basin downstream of three Gorges Dam. *Remote Sensing of Environment*, *152*, 251–269. https://doi.org/10.1016/j.rse.2014.06.004

Yao, F., Livneh, B., Rajagopalan, B., Wang, J., Crétaux, J.-F., Wada, Y., & Berge-Nguyen, M. (2023). Satellites reveal widespread decline in global lake water storage. *Science*, *380*(6646), 743–749. https://doi.org/10.1126/science.abo2812